



## Simulations of a turbulent non-premixed flame using combined dimension reduction and tabulation for combustion chemistry

Zhuyin Ren <sup>a,\*</sup>, Graham M. Goldin <sup>b</sup>, Varun Hiremath <sup>c</sup>, Stephen B. Pope <sup>c</sup>

<sup>a</sup> Department of Mechanical Engineering, University of Connecticut, Storrs, CT 06269, USA

<sup>b</sup> ANSYS, Inc., 10 Cavendish Court, Lebanon, NH 03766, USA

<sup>c</sup> Sibley School of Mechanical and Aerospace Engineering, Cornell University, Ithaca, NY 14853, USA

### HIGHLIGHTS

- ▶ Advanced methods are needed for the use of detailed hydrocarbon chemistry in simulations.
- ▶ We demonstrate a method for accelerating chemistry calculations in CFD.
- ▶ We simulate a bluff-body-stabilized non-premixed turbulent methane/air flame.
- ▶ NO<sub>x</sub> and CO emissions have been accurately and efficiently modeled.
- ▶ Combustion models have no impacts on reduced description of reactive flows.

### ARTICLE INFO

#### Article history:

Received 7 July 2012

Received in revised form 9 August 2012

Accepted 11 August 2012

Available online 1 September 2012

#### Keywords:

Detailed mechanism

Turbulent flames

Dimension reduction

Tabulation

Constrained equilibrium

### ABSTRACT

The use of large chemical mechanisms of hydrocarbon fuels in turbulent flame simulations is computationally expensive due to the large number of chemical species and the wide range of chemical time scales involved. The reduced description of reactive flows in combination with chemistry tabulation can effectively reduce the simulation time when detailed chemical kinetics is employed in multi-dimensional Computational Fluid Dynamics (CFDs). In this study, this approach is applied to simulate a bluff-body-stabilized non-premixed flame with the eddy dissipation concept (EDC) and transported probability density function (PDF) combustion models. In the calculations, the 31 chemical species in the GRI-Mech 1.2 mechanism are partitioned into represented species and unrepresented species. The reactive system is described in terms of a smaller number of represented species instead of the full set of chemical species in the mechanism; and the evolution equations are solved only for the represented species. The *In Situ* Adaptive Tabulation (ISAT) approach is employed to speed the chemistry calculation by tabulating information of the reduced system. The simulations show that a reduced description with 13 represented species and three atomic elements in the unrepresented species agrees well with the full description that has 31 species while achieving a speed-up factor of up to three. Compared to experimental data, the PDF model yields more accurate predictions in the composition fields of upstream locations than EDC. The impact of the reduced description on NO<sub>x</sub> emissions is also studied by performing the full and reduced descriptions of the flame with GRI-Mech 3.0. The study shows that a reduced description with a total 16 represented species, including three nitrogen-containing species, agrees well with the full description and incurs less than 5% error in NO predictions. Moreover, in this study, an efficient initialization procedure is first demonstrated for the CFD calculations with detailed chemistry.

© 2012 Elsevier Ltd. All rights reserved.

## 1. Introduction

Realistic modeling of chemically reactive flows burning hydrocarbon fuels involves a large number of chemical species, which participate in tens to thousands of chemical reactions occurring simultaneously within a complex flow field [1]. For example, a de-

tailed mechanism for iso-octane [2] contains more than eight hundred species that participate in more than three thousand reactions. Currently, it is computationally prohibitive to directly incorporate detailed chemical kinetics in multi-dimensional simulations due principally to the large number of species involved and the wide range of chemical time scales present, although its use is essential for a reliable prediction of ignition and extinction phenomena, and emissions such as CO and NO<sub>x</sub>. To meet this challenge, significant progress has been made in methodologies and

\* Corresponding author. Tel.: +1 860 486 8994; fax: +1 860 486 5088.

E-mail address: [Zhuyin.Ren@engr.uconn.edu](mailto:Zhuyin.Ren@engr.uconn.edu) (Z. Ren).

algorithms that rationally reduce the computational burden imposed by the use of detailed chemical kinetics in CFD [1,3–32]. Among the available techniques, three frequently used in the literature are: the development of skeletal mechanisms from large detailed mechanisms by the elimination of inconsequential species and reactions [9–13]; dimension-reduction techniques [14–27]; and storage/retrieval methodologies such as *in situ* adaptive tabulation (ISAT) [28,29], repro-modeling [30], piecewise implementation of solution mapping (PRISM) [31], and artificial neural networks (ANNs) [32].

In recent years, combined methodologies have also been developed, wherein reduced mechanisms or dimension reduction methods are used in conjunction with storage/retrieval methods [18,33–35]. For example, a reduced description of reactive flows was recently developed by Ren et al. [35] by exploiting, in combination, techniques of dimension reduction and storage retrieval to effectively reduce the computational cost of detailed chemical kinetics in CFD. It can be implemented in a species-transport-equation-based CFD solver or a particle-based (such as PDF methods) CFD solver. In this approach, the full set of  $n_s$  chemical species in mechanism are partitioned into  $n_{rs}$  represented species and  $n_{us}$  unrepresented species (with  $n_{rs} + n_{us} = n_s$ ). A flow solver solves the evolution equations only for the  $n_{rs}$  represented species instead of for the full set of  $n_s$  chemical species. Only when necessary, the  $n_{us}$  unrepresented species are reconstructed assuming that they are in constrained chemical equilibrium. The ISAT method is employed to speed the chemistry calculation by tabulating information of the reduced system. Hence the approach determines and tabulates *in situ* the necessary information of the reduced system based on the  $n_s$ -species detailed mechanism. In [35], the approach was validated in both premixed and non-premixed methane/air laminar flames. With the GRI-Mech 1.2 mechanism consisting of 31 species, with a relatively moderate decrease in accuracy, the reduced descriptions (with 12–16 represented species) achieve an additional speedup factor of up to three compared to the full description with ISAT, which has already achieved at least one order of magnitude speed up compared to the ones without ISAT.

In this work, this reduced description approach is further investigated in turbulent flame calculations in the context of different combustion models. Specifically, reduced descriptions of a bluff-body-stabilized non-premixed turbulent flame [36] are performed with the eddy dissipation concept (EDC) [37] and transported probability density function (PDF) combustion models [38]. The accuracy and efficiency of the reduced descriptions are assessed against the full descriptions in which all the chemical species are transported. Particularly, the impact of the combustion models on the accuracy of the reduced description will be investigated and the impact of reduced description on NOx emission prediction will be quantified. Moreover a computationally efficient initialization procedure is first demonstrated for numerical calculations with detailed chemistry. The outline of the remainder of the paper is as follows. In Section 2, the reduced description of reactive flows with tabulation of chemistry is briefly reviewed. The calculation details and results are reported in Sections 3, and Section 4 provides conclusions.

## 2. Reduced description of reactive flows with tabulation of chemistry

In this section we briefly describe the notions and steps in the reduced description; full details are provided in [35]. We consider a reacting gas-phase mixture consisting of  $n_s$  chemical species, composed of  $n_e$  elements. The thermo-chemical state of the mixture (at a given position and time) is completely characterized by

the pressure  $p$ , the mixture enthalpy  $h$ , and the  $n_s$ -vector  $\mathbf{z}$  of specific moles of the species. (The specific moles of species  $i$  is given as  $z_i = Y_i/w_i$ , where  $Y_i$  and  $w_i$  are the mass fraction and molecular weight of the species  $i$ , respectively. In reactive flow calculations, the species concentrations are governed by two processes: chemical reaction and transport. We consider the important class of solution methods in which a splitting scheme is used, where the chemical reaction and transport processes are accounted for in two separate sub-steps. Due to chemical reactions, the composition  $\mathbf{z}$  evolves in time according to the following set of ordinary differential equations (ODEs):

$$\frac{d\mathbf{z}}{dt} = \mathbf{s}(\mathbf{z}) \quad (1)$$

where  $\mathbf{S}$  is the  $n_s$ -vector of chemical production rates determined by the chemical mechanism used to represent the chemistry.

### 2.1. Reduced representation of chemistry

In the reduced description via dimension reduction, species are decomposed as  $\mathbf{z} = \{\mathbf{z}^r, \mathbf{z}^u\}$ , where  $\mathbf{z}^r$  is an  $n_{rs}$ -vector of “represented” species, and  $\mathbf{z}^u$  is an  $n_{us}$ -vector of “unrepresented” species (with  $n_{rs} + n_{us} = n_s$  and  $n_{rs} < n_s - n_e$ ). The reduced representation of the chemistry is  $\mathbf{r} \equiv \{\mathbf{z}^r, \mathbf{z}^{u,e}\}$ , where  $\mathbf{z}^{u,e}$  is an  $n_e$ -vector giving the specific moles of the elements in the unrepresented species (for atom conservation). The elements in the unrepresented species are needed when reconstructing the unrepresented species using constrained equilibrium. Thus  $\mathbf{r}$  is a vector of length  $n_r = n_{rs} + n_e$ , and the dimension of the system is reduced from  $n_s$  to  $n_r$ . At any time, the reduced representation  $\mathbf{r}$  is related to the full composition  $\mathbf{z}$  by  $\mathbf{r} = \mathbf{B}^T \mathbf{z}$ , where  $\mathbf{B}$  is a known constant  $n_s \times n_r$  matrix which can be determined for a specified set of represented species. The thermo-chemical state of the reduced reactive system is represented by  $\{\mathbf{r}(\mathbf{x}, t); h(\mathbf{x}, t); p(\mathbf{x}, t)\}$ . With assigned thermal and transport properties, the elements in the unrepresented species  $\mathbf{z}^{u,e}$  are treated as “notional” species in the reduced description.

### 2.2. Steps in reduced description

In the reduced description, only the transport equations for the reduced composition  $\tilde{\mathbf{r}} = \{\mathbf{r}; h\}$  are solved. Note that the unrepresented elements  $\mathbf{z}^{u,e}$  do not have chemical reaction source terms. Chemical reactions are separated into a single reaction fractional step, where the effect of chemical reactions on the reduced composition is addressed through “species reconstruction” using constrained equilibrium [16–21] and the evaluation of reaction mapping in the full composition space. Specifically, the change in reduced composition due to chemical reactions is addressed through the following three major steps. The first step is the species reconstruction, i.e. given the initial reduced composition  $\tilde{\mathbf{r}}(0)$ , the initial full composition before reaction, denoted by  $\Phi^{CE}(0) = \{z^{CE}, h, p\}$  is obtained by assuming that the unrepresented species are in constrained chemical equilibrium at the cell (or particle) pressure and enthalpy, subject to the constraints of the represented species and the unrepresented elements. The constrained-equilibrium composition is computed using the CEQ [39] code. The second step is to obtain the reaction mapping. The set of ODEs Eq. (1) (together with the energy variable) is integrated numerically in the full space for a reaction time step  $\Delta t$  to obtain the reaction mapping (i.e. the composition after reaction) of all the species,  $\Phi(\Delta t)$ . The final step is reduction, i.e. from the obtained reaction mapping,  $\Phi(\Delta t)$ , extract the reaction mapping of the reduced composition denoted by  $\mathbf{R}(\tilde{\mathbf{r}}) \equiv \tilde{\mathbf{r}}(\Delta t)$  using  $\mathbf{r} = \mathbf{B}^T \mathbf{z}$ . Note that a different approach for the second step [18,33] is to integrate the rate equations for the constraint potentials, which is more economical than integrating the ODEs (Eq. (1)) directly. In our

implementation, the former approach is adopted for the ease of combining dimension reduction method with ISAT.

In the reduced description with tabulation of chemistry, ISAT [28,29] is employed to accelerate the determination of the reduced composition after reaction. Briefly stated, an ISAT table stores pairs of reduced compositions before and after reaction  $\{\tilde{\mathbf{r}}, \mathbf{R}(\tilde{\mathbf{r}})\}$  together with the gradient matrix  $A_{ij} = \partial R_i / \partial \tilde{r}_j$ , so that given a new query  $\tilde{\mathbf{r}}(0)$  to be evaluated, the corresponding value  $\tilde{\mathbf{r}}(\Delta t)$  can be retrieved from the table with linear approximation (if it is within the user-specified error tolerance). As needed, pairs of values  $\{\tilde{\mathbf{r}}, \mathbf{R}(\tilde{\mathbf{r}})\}$  together with the gradient matrix are added to the table by the above three-step processes. Hence, in the reduced description the reduction/tabulation approach determines and tabulates *in situ* the necessary information about the  $n_r$ -dimensional reduced system based on the  $n_s$ -species detailed mechanism. With the reduced description, given the same specified ISAT storage, the ISAT table with  $n_r$  dimensions is capable of covering more of composition space than is the ISAT tabulation of the full  $n_s$  dimensions. Also, the ISAT retrieval is faster than that in the full description. Consequently, a simulation with the reduced description may initially be not much faster than that with full description due to the extra constrained equilibrium calculations when adding entries in ISAT table, but iterations can be substantially faster at later times when the ISAT table is retrieved.

### 2.3. Specification of represented species

In the present implementation of reduced description, a specified set of represented species is needed as constraints to perform dimension reduction. The specification of represented species is crucial for the accuracy of reduced description [35]. In the current implementation, the represented species can be specified manually or by a more automatic optimal specification [45,46] using the greedy algorithm based on the minimization of the reaction mapping error of a representative combustion process in partially stirred reactors.

## 3. Numerical simulations

In this study, the reduced description with chemistry tabulation is implemented in the CFD package Fluent. It can be used with the EDC, laminar finite rate model or transported PDF model together with detailed/skeletal chemical mechanisms. The reduced description is valid for both premixed and non-premixed flames. Chemical mechanisms are straightforwardly imported through a graphic interface, where the represented species can be specified. The flow solver solves the conservation equations of mass, momentum, energy and species. The transport properties of the notional species can be specified to be constants or to be the arithmetic average of those of all the represented species. The thermodynamic properties of the notional species (i.e. the unrepresented elements) are specified to be those of the corresponding species in standard states except for element C, which is specified to be those of gaseous species C(s). Note that the specification of thermodynamic properties is insignificant if the mixture enthalpy  $h$  is employed to represent energy.

The reduced description approach here is investigated in a bluff-body-stabilized non-premixed turbulent flame, namely HM1 [34] in the context of different combustion models. In this flame, a methane–hydrogen fuel jet is surrounded by a bluff body and a co-flowing air stream. The diameter of the bluff body,  $D_b$ , is 0.05 m, and that of the jet is 0.0036 m. Numerical modeling of this flame has been extensively performed [40–45]. It was found that it is essential for any turbulence model to capture the complex flow structure to describe the flame physics accurately. The flame is

stabilized by recirculation zones near the solid bluff body, with strong turbulent mixing initiating and maintaining the reactions. The emphasis of the simulations in this study is to assess the robustness of reduced description (in the context of different combustion models), to assess the accuracy and efficiency against the full description in which all the chemical species are transported, the impact of the combustion models on the accuracy of the reduced description, and the impact of reduced description on NOx emission predictions. Both full and reduced descriptions of this flame are performed with the EDC model [37] and the PDF model [38], respectively.

The EDC model is a species-transport-equation-based combustion model, which assumes that chemical reactions occur in small scale turbulent structures embedded in CFD cells and calculates a volume fraction of small scale eddies in which the reactions occur. Combustion at the fine scales is assumed to occur as a constant pressure perfectly stirred reactor. It can incorporate detailed chemical mechanisms and turbulence-chemistry interactions in simulations, and is completely different from eddy break-up model. The transported PDF model employed in the calculations is the composition PDF method, which is implemented through a hybrid mesh-particle method based on a finite difference flow solver and a Lagrangian PDF particle method [41]. Specifically, the flow solver computes the velocity vector and passes the mean velocity vector and turbulence quantities to the PDF particles. The information on the fixed finite difference grid points will be interpolated to the Lagrangian particles with varying locations. The particles advance temporally in the physical space following the velocity field and the composition varies due to molecular mixing and chemical reaction. At the end of the particle evolution, density and transport properties are statistically deduced from the particles and fed back to the flow solver for the advancing of the flow fields. PDF methods offer the ability to accurately resolve finite-rate chemistry and the turbulence-chemistry interactions without any assumption.

In this study, the performance of reduced description in the context of these two widely-accepted combustion models is studied in the bluff-body-stabilized turbulent flame.

### 3.1. Simulation settings

The computational domain is illustrated in Fig. 1. With the origin of the co-ordinate system being taken at the center of the fuel jet exit plane, the axisymmetric computational domain extends ten jet diameters upstream. The domain is discretized with a non-uni-

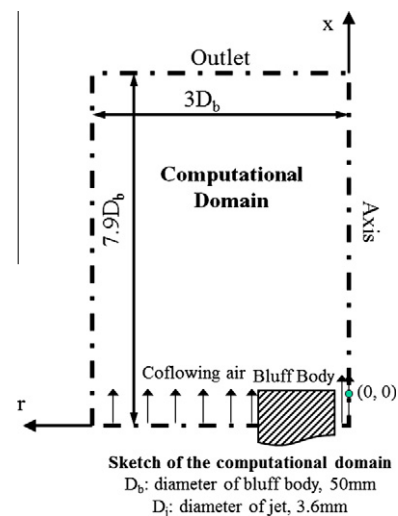


Fig. 1. Sketch of the computational domain.

form Hex mesh of about 45,000 computational cells. The flow solver solves the conservation equations of mass, momentum, turbulence quantities, energy and species with constant transport properties. The chemical mechanism employed is GRI-Mech 1.2 [46] that has four elements, 31 species and 175 reactions. All calculations are performed with the ISAT error tolerance of  $5 \times 10^{-5}$  and the allowed ISAT table size of 500 Mbytes. In the reduced description, the following 13 species are chosen to be the represented species:  $H_2$ , H, O,  $O_2$ , OH,  $CH_3$ ,  $CH_4$ ,  $CO_2$ ,  $CH_2O$ , CO,  $H_2O$ ,  $HO_2$ ,  $N_2$ . Since the element N is fully represented by the species  $N_2$ , only the unrepresented elements C, H and O are considered as notional species denoted as UC, UH, and UO, respectively. This specification of the represented species is obtained using the greedy algorithm based on the minimization of the reaction mapping error of methane/air combustion in a partially stirred reactor [47,48]. Interestingly, the identified represented species are coincidentally identical to the major species in the 13-species reduced mechanism [49] for lean methane–air flame developed from GRI-Mech 1.2, where the major species are the slow species identified using computational singular perturbation [27,28]. The details of the settings are listed in Table 1. For EDC and PDF, default model parameters are employed in the calculations.

### 3.2. Initialization

For simulations with detailed chemical kinetics, the initial solution has significant impact on convergence and computational efficiency. In this work, the characteristic time scale (CTS) model with tabulation of chemical equilibrium [50] is used to generate initial solutions for subsequent calculations. In the initialization phase with CTS, the full set of chemical species are transported and the rate of change of the  $i$ th chemical species in a CFD cell due to chemical reactions is given by:

$$\frac{dz_i}{dt} = -\frac{z_i - z_i^{eq}}{\tau} \quad (2)$$

where  $z_i^{eq}$  is the local instantaneous thermodynamic equilibrium composition, and is  $\tau$  a characteristic time scale determined by both the flow field and chemical time scale [50]. The CTS model implies that species react toward their local chemical equilibrium state over the characteristic time, and is suitable for a wide range of turbulent reactive flows. The chemical equilibrium composition is efficiently evaluated using ISAT (with a large error tolerance of  $1 \times 10^{-3}$  for better efficiency in the initialization phase). For this initialization phase, the whole CFD domain was assigned with pure air of 2000 K at the beginning and it requires about 3000 iterations to establish a realistic flame shape.

Fig. 2 shows the predictions of temperature from both CTS and EDC (full description). As shown, the CTS model yields a realistic initial flame shape for subsequent simulations. For the simulation with EDC, the initialization process by CTS accounts for less than

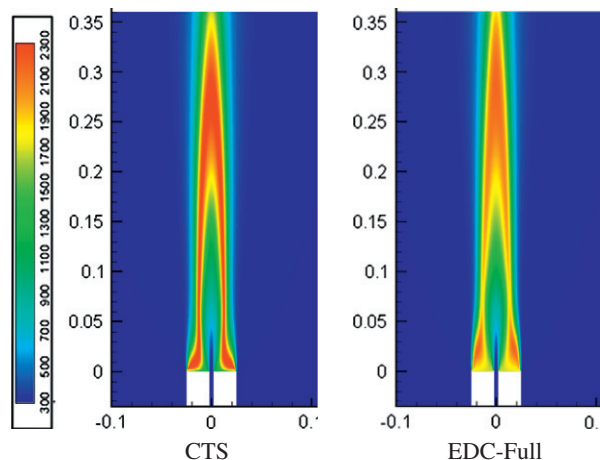


Fig. 2. Contours of Favre mean temperature (K) from CTS and EDC with full description.

0.5% of the whole simulation time. Hence the CTS model is a computationally efficient way to provide good initial solutions for calculations of general reactive flows with detailed chemical kinetics.

### 3.3. Results

In this study, the loss in accuracy as well as the gain in run-time of the reduced description is reported by comparing against the full description with ISAT. Plots are presented for temperature, OH and NO mass fractions. The OH species is representative of the important intermediate species. The impact of the reduced description on the convergence of the simulations is also reported.

Figs. 3 and 4 show the contours of temperature and radical OH from the full and reduced descriptions with EDC and PDF, respectively. As shown, for each model, the reduced description with 13 represented species agrees well with the full description. For the two combustion models, EDC predicts a thinner flame with a higher flame temperature than PDF since the EDC model does not account for scalar fluctuations.

A more quantitative comparison between the simulations and experimental data is given in Figs. 5 and 6, which show the radial profiles of temperature and OH at different axial locations. The reduced description primarily involves two errors: (i) the *tabulation* error due to the use of ISAT; and (ii) the *reduction* error due to the use of fewer represented species. The tabulation error is controlled by the specified ISAT error tolerance, and the reduction error is controlled by the number of represented species used in the reduced description. A thorough study of the two errors for methane premixed combustion in a partially stirred reactor is performed in [48]. Here we simply assess the reduction error in reduced description by comparing against the full description.

Table 1

Numerical conditions selected for computing the bluff-body-stabilized non-premixed turbulent flame.

Domain	Axisymmetric
Solver	Pressure-based with implicit formulation
Turbulence model	Standard $k-\epsilon$ with $C_\mu = 0.09$ , $C_{\epsilon 1} = 1.6$ , $C_{\epsilon 2} = 1.92$ , $\sigma_k = 1.0$ , $\sigma_\epsilon = 1.3$ , energy Prandtl number 0.85, turbulent Schmidt number 0.7
Mixing model	EMST with $C\phi = 2.0$
Number of particle per cell	20
Wall treatment	Low Reynolds number model
Discretization schemes	Standard for pressure; SIMPLE for pressure-velocity coupling; second order upwind for all the quantities
Material	Incompressible ideal gas; mixing law for $C_p$ ; mass weighted mixing law for thermal conductivity and viscosity; kinetic theory for mass diffusivities
$H_2/CH_4$ Fuel stream (1:1 in volume)	Axial velocity 118 m/s with turbulent intensity 10% and a hydraulic diameter of 0.0036 m; $T = 300$ K
Coflowing air stream	Velocity profile from experimental data with turbulent intensity 10% and a hydraulic diameter of 0.25 m; $T = 300$ K

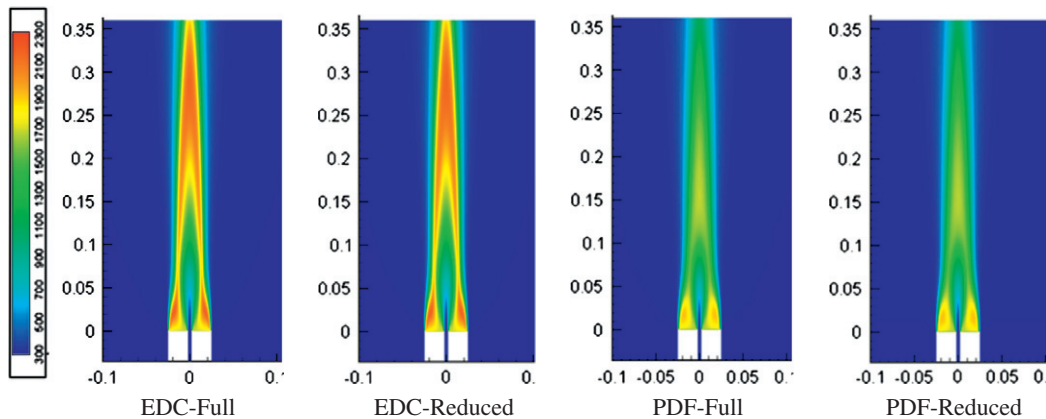


Fig. 3. Contours of Favre mean temperature from the full and reduced descriptions with EDC and PDF, respectively.

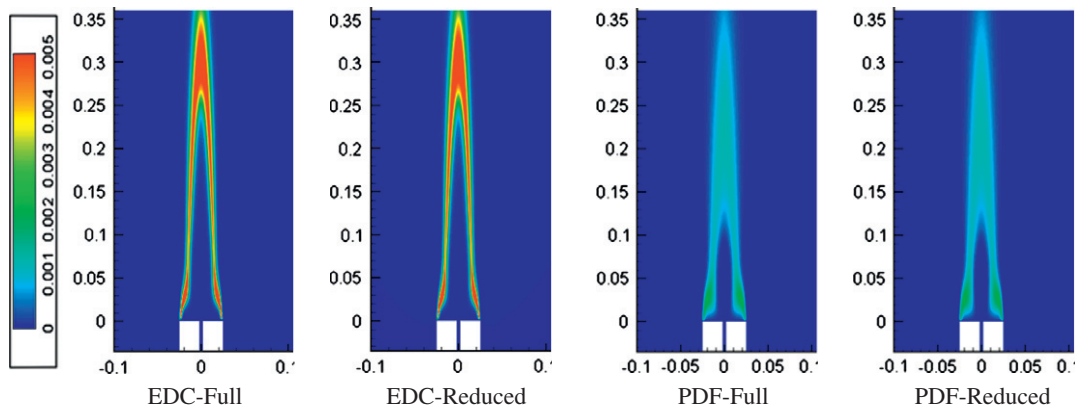


Fig. 4. Contours of Favre mean OH mass fraction from the full and reduced descriptions with EDC and PDF, respectively.

The most important observation is that for each combustion model, except the slight discrepancy (less than 0.5%) at the location of  $x/D_b = 0.26$ , there is no noticeable difference between the full and reduced descriptions. This agreement is much better than those in non-premixed methane/air laminar flame test [35], where the reduced descriptions (with 12–16 represented species) over-predict the peak temperature about 40–60 K. Compared to experimental data, EDC significantly over-predicts the temperature and OH fields. In contrast, the PDF model yields more accurate predictions in the upstream locations. But the prediction deteriorates for the downstream locations due to the over-prediction of turbulent mixing. It is worth mentioning that better agreement between simulations and experimental data have been reported in [40–45] with more sophisticated turbulence and combustion models such as large eddy simulation [43] or joint velocity–frequency–composition PDF method [44]. The focus of this study is the quantification of the accuracy of the reduced description compared to the full description with the same model settings. The impact of the turbulence model and parameters on the mixing prediction is beyond the scope of this study.

The distribution of the unrepresented elements (treated as notional species) is shown in Fig. 7. Two important observations are as follows. The unrepresented elements are small in quantity. As shown, the peak value of the mass fraction of the largest unrepresented element (carbon) is less than 0.03, which is less than 4% of the value of carbon at fuel inlet. Notice that the mass fraction of methane at fuel inlet is 0.889. The unrepresented elements are localized in the flame region. For all other regions, they are close to zero since all the elements exist in the major reactants or products.

The unrepresented species in the reduced description can be reconstructed, assuming that they are in constrained chemical equilibrium. Fig. 8 shows the mass fraction of  $H_2O_2$  from both the full and reduced descriptions. (The species  $H_2O_2$  is an unrepresented species in the reduced description.) Large differences are observed in both the magnitude and the shape. As discussed in [47,48], there are two types of errors associated with dimension reduction in the reduced description: the species reconstruction error and the reaction mapping error. The species reconstruction error is the error in reconstructing the full composition (compared to full description) given a reduced composition before the reaction step, and the reaction mapping error is the error in the reaction mapping (compared to full description) obtained after the reaction time step starting from the reconstructed composition. Both the species reconstruction and reaction mapping errors depend on the specification of represented species. It was observed that, given a value of  $n_{rs}$ , the set of  $n_{rs}$  represented species that minimize the above two individual errors is different [47]. As far as the accuracy of a reduced description is concerned, the primary interest is to minimize the reaction mapping error. Recall that the specification of represented species in this study was based on the minimization of the reaction mapping error of methane/air combustion in a partially stirred reactor [47,48]. It is not surprising to see a discrepancy in the reconstructed unrepresented species with low concentrations. Actually, as found out in [47], to minimize the species reconstruction error, the optimal specification of the represented species is  $H_2$ ,  $H$ ,  $O$ ,  $O_2$ ,  $OH$ ,  $CH_3$ ,  $CH_4$ ,  $CO_2$ ,  $CH_2O$ ,  $N_2$ ,  $CH_3OH$ ,  $C_2H_4$ ,  $C_2H_6$ . (Notice that the last three species  $CH_3OH$ ,  $C_2H_4$ ,  $C_2H_6$  are replacing  $CO$ ,  $H_2O$ ,  $HO_2$  used in this study.)

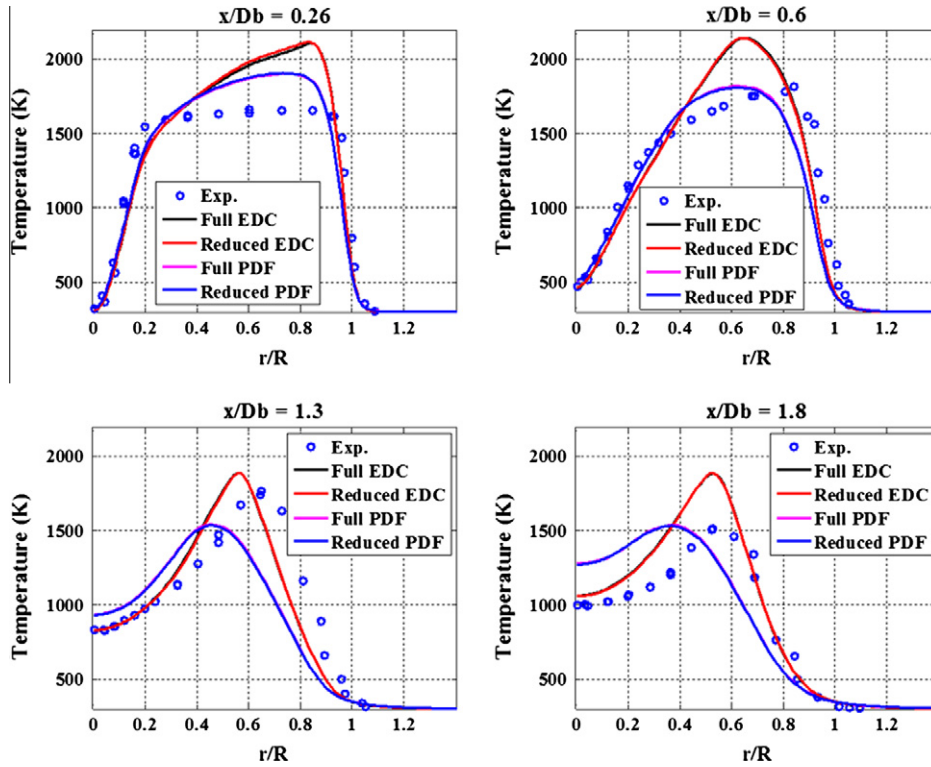


Fig. 5. Radial profiles of Favre mean temperature at different axial locations (experiment:  $\circ$ ). The black and red lines are on top of each other; the blue and magenta lines are on top of each other. (For interpretation of the references to color in this figure legend, the reader is referred to the web version of this article.)

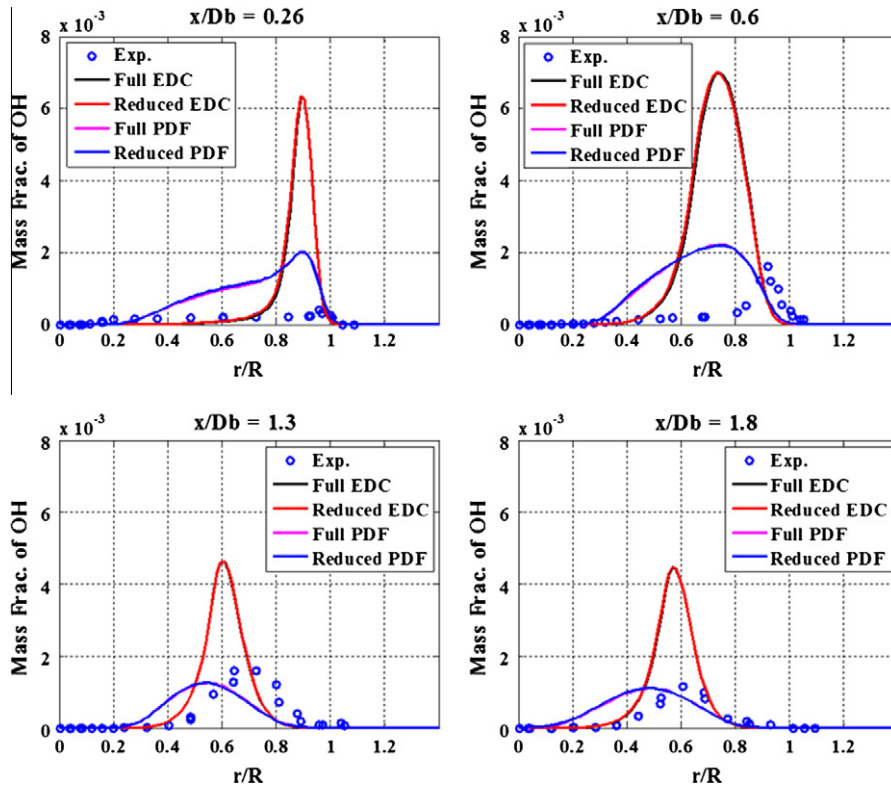


Fig. 6. Radial profiles of Favre mean OH mass fraction at different axial locations (experiment:  $\circ$ ). Black and red lines are on top of each other; blue and magenta lines are on top of each other. (For interpretation of the references to color in this figure legend, the reader is referred to the web version of this article.)

The observed discrepancy in unrepresented species also implies that minor species are not necessarily in constrained equilibrium

(with the current specification of represented species). This is not contradicting the picture that in a reactive flow compositions lie

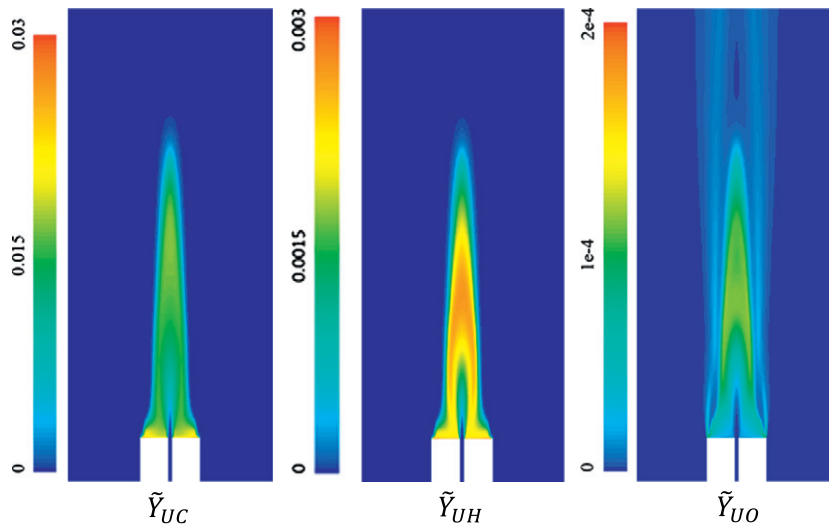


Fig. 7. Contours of Favre mean mass fraction of the notional species (unrepresented elements) UC, UH and UO, respectively from the reduced description with EDC.

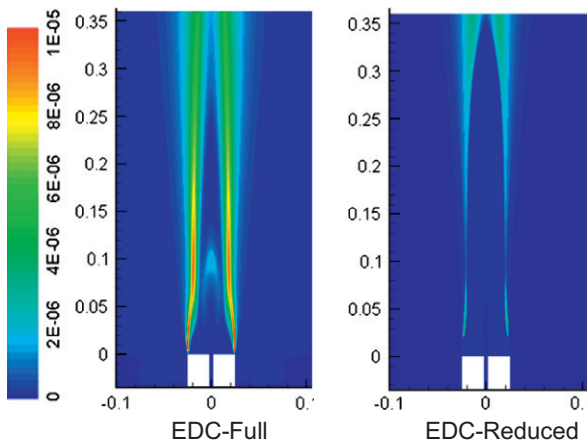


Fig. 8. Contours of Favre mean  $\text{H}_2\text{O}_2$  mass fraction from the full and reduced descriptions with EDC. In the reduced description,  $\text{H}_2\text{O}_2$  is an unrepresented species.

on an intrinsic low-dimensional manifold due to fast chemical time scales. Recognizing the fact that the constrained equilibrium (CE) manifold highly depends on the selection of the represented species, the observed discrepancy only implies the CE manifold (associated with the current specification of represented species) is not a good approximation to the intrinsic low-dimensional manifold. In other words, the reconstructed unrepresented species contain large reconstruction errors. The fact that the represented species in this study are identical to the major species in the 13-species reduced mechanism [49] implies that the species reconstruction error can potentially be improved using other species reconstruction methods like ICE-PIC [24].

As shown in the results (see Figs. 3–6), a large error in the reconstructed unrepresented species may not necessarily have a significant effect on the represented species of concern. This is due to the fact that, in our reduced description, the reconstructed full composition is only used as the initial condition to the full set of ODEs governing the reaction fractional step. Due to the wide range of chemical time scales, all solution trajectories from different initial conditions quickly relax toward the intrinsic low dimensional attracting manifold. Hence the effect of any inaccuracy in the initial condition is likely to be quickly damped out during the reaction fractional step if the unrepresented species are associated

with the fast time scales. This is the case recalling that the represented species are identical to the slow major species in the 13-species reduced mechanism [49].

The impact of reduced description on the convergence of the simulation is examined. It is observed that the reduced description has no significant impact on the convergence. Starting from the CTS solution, the convergence processes of the full and reduced descriptions are similar. Also in the reduced description, the convergence of the notional species (unrepresented elements) is similar to those of represented species.

In this study, starting from the CTS solution the flame calculations require about 1500 iterations for EDC and 3000 iterations for PDF to converge, respectively. Compared to the full description with ISAT, the reduced descriptions achieve additional computational speed-up by solving fewer transport equations and faster ISAT retrieving. In this study, with the relatively small GRI-Mech 1.2 mechanism, compared to the full description with ISAT, the reduced description achieves a speedup factor of 1.8 and 3.2 with EDC and PDF, respectively. It is worth mentioning that the full description in this study has already achieved significant speed-up in the chemistry calculations by ISAT. The efficiency reported here is the additional computational gain achieved by the reduced description. The number reported is the overall speed-up of the whole simulation, not only the chemistry calculation.

### 3.4. Effect of reduced description on NO<sub>x</sub> emission

In this study, to evaluate the impact of the reduced description on NO<sub>x</sub> prediction, the full and reduced descriptions of the flame with the EDC model are performed with GRI-Mech 3.0 [51] that contains NO<sub>x</sub> chemistry. The calculations are performed with the ISAT error tolerance of  $2 \times 10^{-5}$  and the allowed ISAT table size of 500Mbytes. The use of smaller ISAT error tolerance in these two simulations is to reduce the tabulation error incurred for the NO<sub>x</sub> species. In the reduced description, in addition to  $\text{H}_2$ ,  $\text{H}$ ,  $\text{O}$ ,  $\text{O}_2$ ,  $\text{OH}$ ,  $\text{CH}_3$ ,  $\text{CH}_4$ ,  $\text{CO}_2$ ,  $\text{CH}_2\text{O}$ ,  $\text{CO}$ ,  $\text{H}_2\text{O}$ ,  $\text{HO}_2$ ,  $\text{N}_2$ , species  $\text{NH}_3$ ,  $\text{NO}$ ,  $\text{HCN}$  are added to the represented species. The unrepresented elements C, H, O, and N are considered as notional species denoted as UC, UH, UO, and UN respectively. The details of the settings are the same as listed in Table 1. Fig. 9 shows the prediction of NO from both reduced and full descriptions. As may be seen, the reduced description agrees well with the full description and incurs less than 5% reduction error.

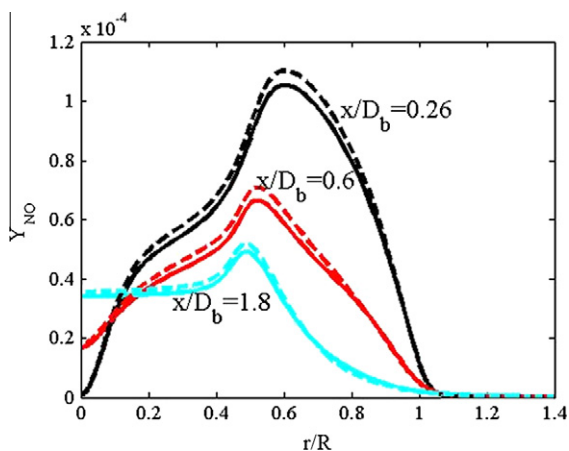


Fig. 9. Radial profiles of Favre mean NO mass fraction at different axial locations. Solid line: full description; dashed line: reduced description.

#### 4. Conclusion

The reduced description with chemistry tabulation can effectively reduce the computational cost of detailed chemical kinetics in CFD. It can be implemented in a species-transport-equation-based CFD solver or a particle-based (such as PDF methods) CFD solver. In this study, this approach is investigated in a bluff-body-stabilized non-premixed turbulent flame. Specifically, a reduced description with 13 represented species is used to perform calculation of this flame with the EDC model and the PDF model. To facilitate the simulations with detailed chemical kinetics, an efficient initialization procedure by the CTS model is demonstrated to generate realistic initial solutions.

The results show that, for each combustion model, the reduced description with 13 represented species agrees well with the full description. Except for the slight discrepancy (less than 0.5%) at one upper-stream location, there is no noticeable difference between the full and reduced descriptions. With the relatively small GRI-Mech 1.2 mechanism, compared to the full description with ISAT, the reduced description achieves a speedup factor of 1.8 and 3.2 with EDC and PDF, respectively. The study also shows that the reduced description has no impact on the convergence of simulations. The convergence of the notional species (unrepresented elements) is similar to those of represented species.

The simulations also show that EDC predicts a thinner flame with a higher flame temperature than PDF. Compared to experimental data, EDC significantly over-predicts the temperature and OH fields. In contrast, the PDF model yields more accurate predictions in the upstream locations. But the prediction deteriorates for the downstream locations due to the over-prediction of turbulent mixing with the selected turbulence model and parameters.

The impact of the reduced description on NO<sub>x</sub> emission is studied by performing the full and reduced descriptions of the flame with GRI-Mech 3.0. The study shows that a reduced description (with a total 16 represented species including the three NO, NH<sub>3</sub>, HCN nitrogen-containing species) agrees well with the full description and incurs less than 5% error in NO prediction.

#### Acknowledgement

This work is supported in part by Department of Energy under Grant DE-FG02-90ER. SBP has a financial interest in Ithaca Combustion Enterprise, LLC., which has licensed the software ISAT-CK and CEQ used in this work.

#### References

- [1] Law CK. Combustion at a crossroads: status and prospects. *Proc Combust Inst* 2007;31:1–29.
- [2] Curran HJ, Gaffuri P, Pitz WJ, Westbrook CK. A comprehensive modelling study of iso-octane oxidation. *Combust Flame* 2002;129:253–80.
- [3] Griffiths JF. Reduced kinetic models and their application to practical combustion systems. *Prog Energy Combust Sci* 1995;21:25–107.
- [4] Tomlin AS, Tuányi T, Pilling MJ. *Comprehensive chemical kinetics 35*, in low temperature combustion and autoignition. Amsterdam: Elsevier; 1997. p. 293–437.
- [5] Okino MS, Mavrouniotis ML. Simplification of mathematical models of chemical reaction systems. *Chem Rev* 1998;98:391–408.
- [6] Lu TF, Law CK. Toward accommodating realistic fuel chemistry in large-scale computations. *Prog Energy Combust Sci* 2009;35:192–215.
- [7] Pope SB, Ren Z. Efficient implementation of chemistry in computational combustion. *Flow Turbul Combust* 2009;82:437–53.
- [8] Goldin GM, Ren Z, Zhirovic S. A cell agglomeration algorithm for accelerating detailed chemistry in CFD. *Combust Theor Model* 2009;13:721–39.
- [9] Lu TF, Law CK. A directed relation graph method for mechanism reduction. *Proc Combust Inst* 2005;30:1333–41.
- [10] Valorani M, Creta F, Goussis DA, Lee JC, Najm HN. An automatic procedure for the simplification of chemical kinetic mechanisms based on CSP. *Combust Flame* 2006;146:29–51.
- [11] Pepiot P, Pitsch H. An efficient error-propagation-based reduction method for large chemical kinetic mechanisms. *Combust Flame* 2008;154:67–81.
- [12] Luo Z, Lu TF, Maciaszek M, Som S, Longman D. A reduced mechanism for high-temperature oxidation of biodiesel surrogates. *Energy Fuel* 2010;24:6283–93.
- [13] Luo Z, Plomer M, Lu TF, Som S, Longman DE, Sarathy SM, et al. A reduced mechanism for biodiesel surrogates for compression ignition engine applications. *Fuel* 2012;99:143–53.
- [14] Smooke MD, editor. *Reduced kinetic mechanisms and asymptotic approximations for methane–air flames*. Berlin: Springer; 1991.
- [15] Chen JY. A general procedure for constructing reduced reaction mechanisms with given independent relations. *Combust Sci Technol* 1988;57:89–94.
- [16] Keck JC, Gillespie D. Rate-controlled partial-equilibrium method for treating reacting gas mixtures. *Combust Flame* 1971;17:237–41.
- [17] Keck JC. Rate-controlled constrained-equilibrium theory of chemical reactions in complex systems. *Prog Energy Combust Sci* 1990;16:125–54.
- [18] Tang Q, Pope SB. Implementation of combustion chemistry by *in situ* adaptive tabulation of rate-controlled constrained equilibrium manifolds. *Proc Combust Inst* 2002;29:1411–7.
- [19] Tang Q, Pope SB. A more accurate projection in the rate-controlled constrained-equilibrium method for dimension reduction of combustion chemistry. *Combust Theor Model* 2004;8:255–79.
- [20] Jones WP, Rigopoulos S. Rate-controlled constrained equilibrium: formulation and application to nonpremixed laminar flames. *Combust Flame* 2005;142:223–34.
- [21] Janbozorgi M, Ugarte S, Metghalchi H, Keck JC. Combustion modeling of mono-carbon fuels using the rate-controlled constrained-equilibrium method. *Combust Flame* 2009;156:1871–85.
- [22] Gorban AN, Karlin IV. Method of invariant manifold for chemical kinetics. *Chem Eng Sci* 2003;58:4751–68.
- [23] Maas U, Pope SB. Simplifying chemical kinetics: intrinsic low-dimensional manifolds in composition space. *Combust Flame* 1992;88:239–64.
- [24] Ren Z, Pope SB, Vladimirovsky A, Guckenheimer JM. The invariant constrained equilibrium edge preimage curve method for the dimension reduction of chemical kinetics. *J Chem Phys* 2006;124:114111.
- [25] Lam SH. Using CSP. To understand complex chemical kinetics. *Combust Sci Technol* 1993;89:375–404.
- [26] Lam SH, Goussis DA. The CSP method for simplifying kinetics. *Int J Chem Kinet* 1994;26:461–86.
- [27] Lu TF, Ju Y, Law CK. Complex CSP for chemistry reduction and analysis. *Combust Flame* 2001;126:1445–55.
- [28] Pope SB. Computationally efficient implementation of combustion chemistry using *in situ* adaptive tabulation. *Combust Theor Model* 1997;1:41–63.
- [29] Lu L, Pope SB. An improved algorithm for *in situ* adaptive tabulation. *J Comput Phys* 2009;228:361–86.
- [30] Tuányi T. Parameterization of reaction mechanisms using orthonormal polynomials. *Proc Combust Inst* 1994;25:949–55.
- [31] Bell JB, Brown NJ, Day MS, Frenklach M, Grcar JF, Propp RM, et al. Scaling and efficiency of prism in adaptive simulations of turbulent premixed flames. *Proc Combust Inst* 2000;28:107–13.
- [32] Christo FC, Masri AR, Nebot EM. Artificial neural network implementation of chemistry with pdf simulation of H<sub>2</sub>/CO<sub>2</sub> flames. *Combust Flame* 1996;106:406–27.
- [33] Tang Q, Xu J, Pope SB. PDF calculations of local extinction and NO production in piloted-jet turbulent methane/air flames. *Proc Combust Inst* 2000;28:133–9.
- [34] Ren Z, Hiremath V, Pope SB. Dimension reduction and tabulation of combustion chemistry using ICE-PIC and ISAT. In: 6th US national combustion meeting. Ann Arbor, Michigan; May 17–20, 2009.
- [35] Ren Z, Goldin GM, Hiremath V, Pope SB. Reduced description of reactive flows with tabulation of chemistry. *Combust Theor Model* 2011;15(6):827–48.

- [36] Dally BB, Masri AR, Barlow RS, Fietchner GJ. Instantaneous and mean compositional structure of bluff-body stabilized nonpremixed flames. *Combust Flame* 1998;114:119–48.
- [37] Gran IR, Magnussen BF. A numerical study of a bluff-body stabilized diffusion flame. Part 2. Influence of combustion modelling and finite-rate chemistry. *Combust Sci Technol* 1996;119:191–217.
- [38] Pope SB. PDF methods for turbulent reactive flows. *Prog Energy Combust Sci* 1985;11:119–92.
- [39] Pope SB. Gibbs function continuation for the stable computation of chemical equilibrium. *Combust Flame* 2004;139:222–6.
- [40] Kim SH, Huh KY. Use of the conditional moment closure model to predict NO formation in a turbulent CH<sub>4</sub>/H<sub>2</sub> flame over a bluff-body. *Combust Flame* 2002;130:94–111.
- [41] Muradoglu M, Liu K, Pope SB. PDF modeling of a bluff-body stabilized turbulent flame. *Combust Flame* 2003;132:115–37.
- [42] Dally BB, Fletcher DF, Masri AR. Flow and mixing fields of turbulent bluff-body jets and flames. *Combust Theor Model* 1998;2:193–219.
- [43] Raman V, Pitsch H. Large-eddy simulation of a bluff-body-stabilized non-premixed flame using a recursive filter-refinement procedure. *Combust Flame* 2005;142:329–47.
- [44] Liu K, Pope SB, Caughey DA. Calculations of bluff-body stabilized flames using a joint probability density function model with detailed chemistry. *Combust Flame* 2005;141:89–117.
- [45] Zhu M, Han X, Ge H, Chen Y. Simulation of bluff body stabilized flows with hybrid RANS and PDF method. *Acta Mech Sin* 2007;23:263–73.
- [46] Frenklach M, Wang H, Goldenberg M, Smith GP, Golden DM, Bowman CT, Hanson RK, Gardiner WC, Lissianski V. GRI-Mech: an optimized detailed chemical reaction mechanism for methane combustion. Gas research institute topical report. Chicago: Gas Research Institute; 1995.
- [47] Hiremath V, Ren Z, Pope SB. A greedy algorithm for species selection in dimension reduction of combustion chemistry. *Combust Theor Model* 2010;14:619–52.
- [48] Hiremath V, Ren Z, Pope SB. Combined dimension reduction and tabulation strategy using ISAT-RCCE-GALI for the efficient implementation of combustion chemistry. *Combust Flame* 2011;158:2113–27.
- [49] Sankaran R, Hawkes ER, Chen JH, Lu TF, Law CK. Structure of a spatially developing turbulent lean methane–air Bunsen flame. *Proc Combust Inst* 2007;31:1291–8.
- [50] Ren Z, Goldin GM. An efficient time scale model with tabulation of chemical equilibrium. *Combust Flame* 2011;158:1977–9.
- [51] Smith GP, Golden DM, Frenklach M, Moriarty NW, Eiteneer B, Goldenberg M, Bowman CT, Hanson RK, Song S, Gardiner WC, Lissianski VV, Qin Z. <<http://www.me.berkeley.edu/gri-mech/>>.